

A Wideband Frequency Selective Surface Reflector for 4G/X-Band/Ku-Band

Sarika^{1, *}, Malay R. Tripathy¹, and Daniel Ronnow²

Abstract—A Frequency Selective Surface (FSS) reflector with wideband response for 4G/X-band/Ku-band is proposed. The wideband FSS reflector consists of cascaded dual-layer patch FSS which is etched on separate layers of FR4 substrate. The targeted frequency range is 5–16 GHz. A wide stopband of 10.4 GHz (100% percent bandwidth) is obtained with two layers in cascade. The Equivalent Circuit (EC) method is used to approximate the simulated results. An extensive parametric study is also carried out to understand the effect of various combinations of FSS layers and their disposition. A panel of final FSS is fabricated where measured and simulated results agree well.

1. INTRODUCTION

Frequency Selective Surfaces (FSSs) are a class of spatial filters which are composed of periodic structures in two-/three-dimensions. FSSs are able to provide wideband structures which can act as either band-pass or band-stop filters to a certain frequency range [1–3]. Various studies have been carried out in the past to prove the properties/characteristics of FSS. In [3], a dual-polarized antenna loading FSS is proposed for 5G WLAN (Wireless Local Area Network) applications. The bandwidth of the antenna increases by 40% with gain improvement of 5.6 dBi. A wideband FSS with a sharp band edge is presented in [4], where the periodic cell includes a mushroom-like cavity, and four L-type slots are etched on the top and bottom of the cavity. The FSS operates in X-band. Another way of achieving wideband is presented in [5], where two layers are cascaded to obtain a band-stop in 4–7 GHz. The bandwidth shows an increase of 56%. In [6], a wideband E-shaped microstrip patch antenna is designed for high speed 5G applications. A millimeter-wave application FSS is proposed in [7], where a stopband of 30 GHz is obtained. Reduction of mutual coupling in MIMO (Multiple Input Multiple Output) antenna is obtained through this. In [8], interweaving technique of FSS is used to obtain wideband and size reduction. Focus of this design is to provide shielding in indoor applications. A wideband high directive aperture coupled microstrip antenna is designed in [9] by using an FSS superstrate layer. A tunable FSS for electromagnetic shielding application in frequency range of 3.5–5.8 GHz is studied in [10] for Wimax and WLAN applications. Similarly, in [11–13], a wideband FSS structure is obtained for EMC (Electromagnetic Compatibility) purpose, extended bandwidth backing reflector functions and EBG (Electromagnetic Band Gap) antenna, respectively. In [15], the use of FSS with multi-fractal geometry is investigated. The proposed structure in [15] is easy to implement and produces multiple frequency ratios between adjacent bands. In [16], a 3D FSS is designed for wide stopband which uses a horn shape to enhance the bandwidth properties of FSS. Angular stability is also discussed to show that the wide stopband is achieved with nearly unchanged angular stability of frequency response. In [17], a cascaded circular polarization FSS is presented which has good wideband rejection properties. Genetic Algorithm method is used to analyze the FSS.

Received 9 January 2018, Accepted 8 February 2018, Scheduled 17 February 2018

* Corresponding author: Sarika (sarikauppal@gmail.com).

¹ Department of Electronics and Communication Engineering, ASET, Amity University, Uttar Pradesh, Noida, India. ² Department of Electronics, Mathematics and Natural Sciences, University of Gavle, Gavle, Sweden.

In this paper, a dual-layer wideband frequency selective surface reflector is proposed for 4G/X-band/Ku-band. The design has three layers, which are studied independently; afterwards the combinations of three layers are shown to have wideband reflector property. A comprehensive parametric study is carried out to validate the structure. The panel of FSS fabricated agrees well with the simulation results. This paper is organized as follows. Section 2 presents FSS unit cell design and its equivalent circuit analysis. Section 3 shows parametric study carried out on the design. Section 4 discusses the fabricated design and its results. Section 5 concludes the research work.

2. FSS UNIT CELL DESIGN & ANALYSIS

In order to obtain a wideband FSS reflector, three-layer FSS geometry is used with different unit cells of periodicity 15 mm in both x - and y -directions as shown in Fig. 1. The dimensions (in mm) of unit cells

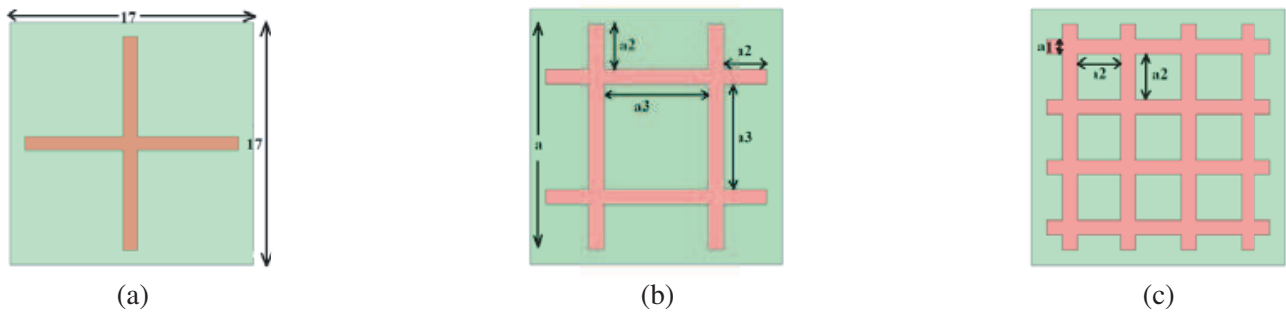


Figure 1. Unit cells of (a) layer I, (b) layer II, (c) layer III.

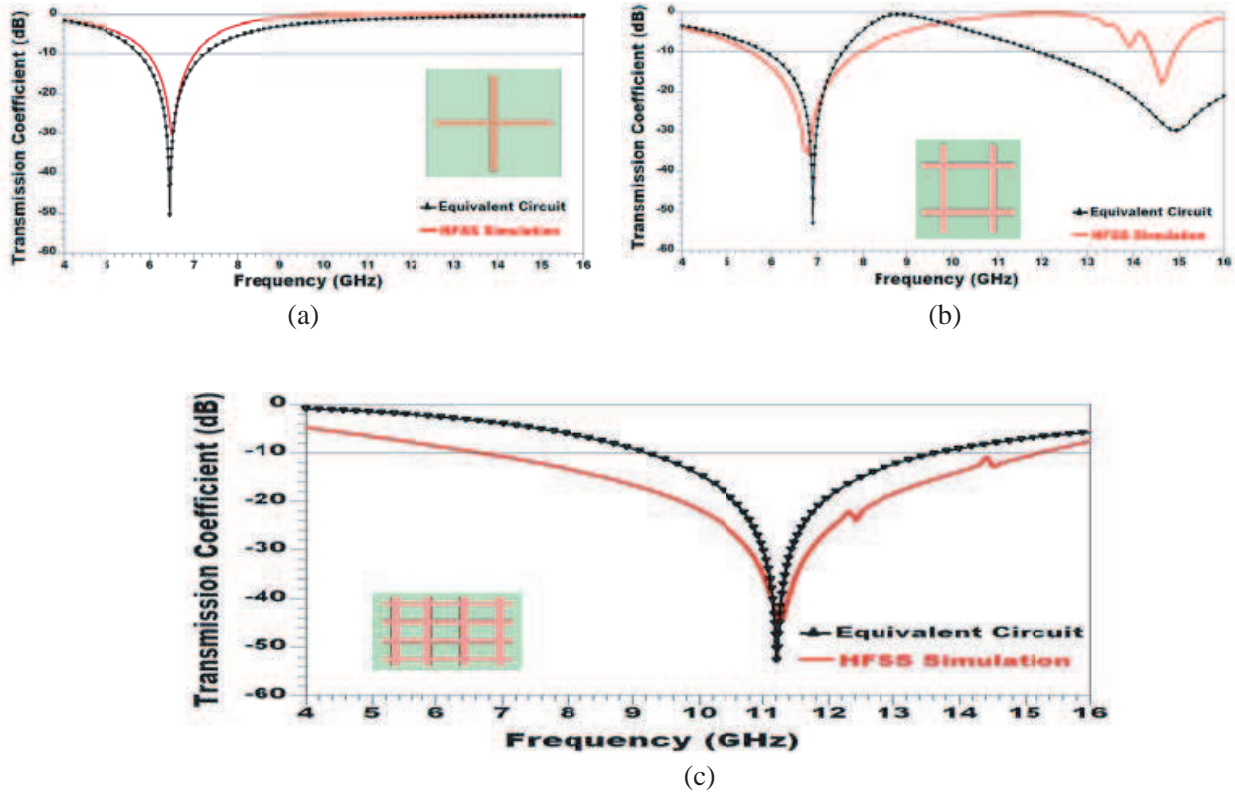


Figure 2. Transmission coefficient (HFSS and equivalent circuit) of (a) layer I, (b) layer II, (c) layer III.

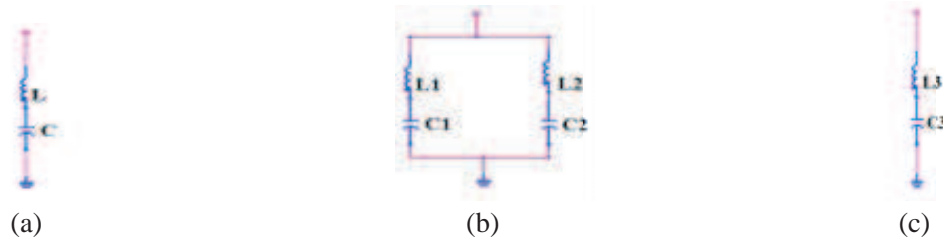


Figure 3. Equivalent circuit model for unit cells of (a) layer I, (b) layer II, (c) layer III.

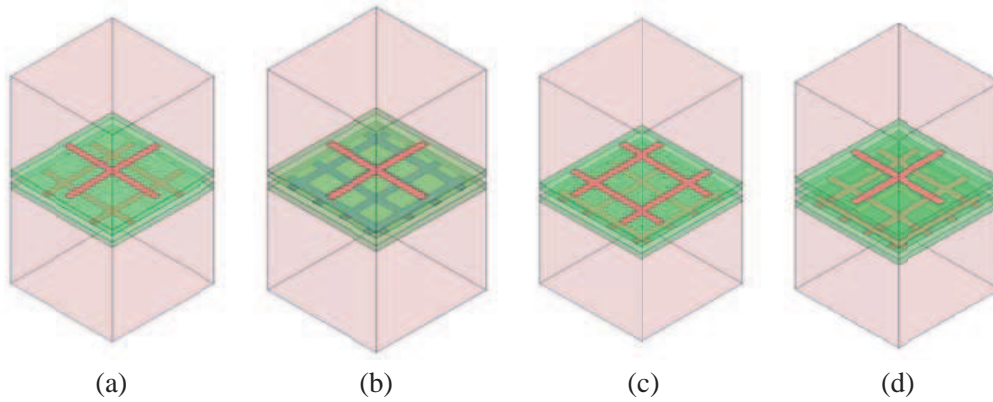


Figure 4. Cascaded combinations of (a) layer I-II, (b) layer I-III, (c) layer II-III, (d) layer I-II-III.

are $a = 15$, $a_1 = 1$, $a_2 = 3$ and $a_3 = 7$. Layer I is a cross dipole shape with dimensions $15 \text{ mm} \times 15 \text{ mm}$. In layer II and layer III, the arm lengths a_2 and a_3 are approximated using Equation (1) to get dual bands and resonance in X-band (8–12 GHz), respectively [5]. In Equation (1), c_0 = velocity of light in free space, f is the resonating frequency, and ϵ_r is the relative permittivity of the substrate used. Each layer is designed on a separate FR4 substrate with $\epsilon_r = 4.4$, loss tangent = 0.002 and height = 1.6 mm. The transmission coefficients of each layer obtained using FEM magnetic solver HFSS software are studied as shown in Fig. 2. A stopband with central frequency 6.4 GHz is obtained with layer I with a bandwidth of 1.1 GHz. Layer II resonates at dual bands at 6.8 GHz and 14.6 GHz. The bandwidth obtained in this case is 2.4 GHz and 600 MHz, respectively. In layer III, the resonating frequency shifts to higher side specifically at 11.3 GHz generating a wide stopband of 8.6 GHz. Equivalent circuit models of unit cells for layers I, II and III are shown in Fig. 3. Layer I is modeled as a series combination of an inductor and capacitor (LC), layer II as parallel combination of two such series resonators (L_1, C_1 and L_2, C_2) and layer III as series L_3, C_3 combination. Their results using Advanced Design System (ADS) tool are compared with simulation results (Fig. 2). They are in agreement with each other. The values of various parameters are $L = 0.016 \mu\text{H}$, $C = 0.038 \text{ pf}$, $L_1 = 0.014 \mu\text{H}$, $C_1 = 0.038 \text{ pf}$, $L_2 = 0.003 \mu\text{H}$, $C_2 = 0.038 \text{ pf}$, $L_3 = 0.005 \mu\text{H}$, $C_3 = 0.0038 \text{ pf}$. In order to obtain a wider stopband, different cascaded combinations of three layers are used. The spacing between them is kept at 1 mm as in Fig. 4. When layer I and layer II are cascaded, dual stopbands are produced, which provide maximum stopband of 3.6 GHz around central frequency of 7.7 GHz. Cascading of layer I and layer III results in wide stopband of 7.6 GHz around central frequency of 10.6 GHz. Layer II and layer III in cascade push the wideband to higher value of 10.4 GHz. However, cascading of layer I-II-III shows a dip in stopband by a factor of 1.4 GHz. Fig. 5 represents the transmission coefficients of all the layers in various combinations. Table 1 summarizes the various parameters calculated from every layer/combination. It can be seen that the combination of layer II-III acts as the best reflector of 4G/X-band/Ku-band with 10.4 GHz bandwidth (percentage bandwidth = 100%) out of all investigated designs.

Figure 6 shows the surface current distribution on unit cells of layer I, layer II and layer III at their respective resonating frequencies. In layer I, the current flows on the horizontal arm of the unit

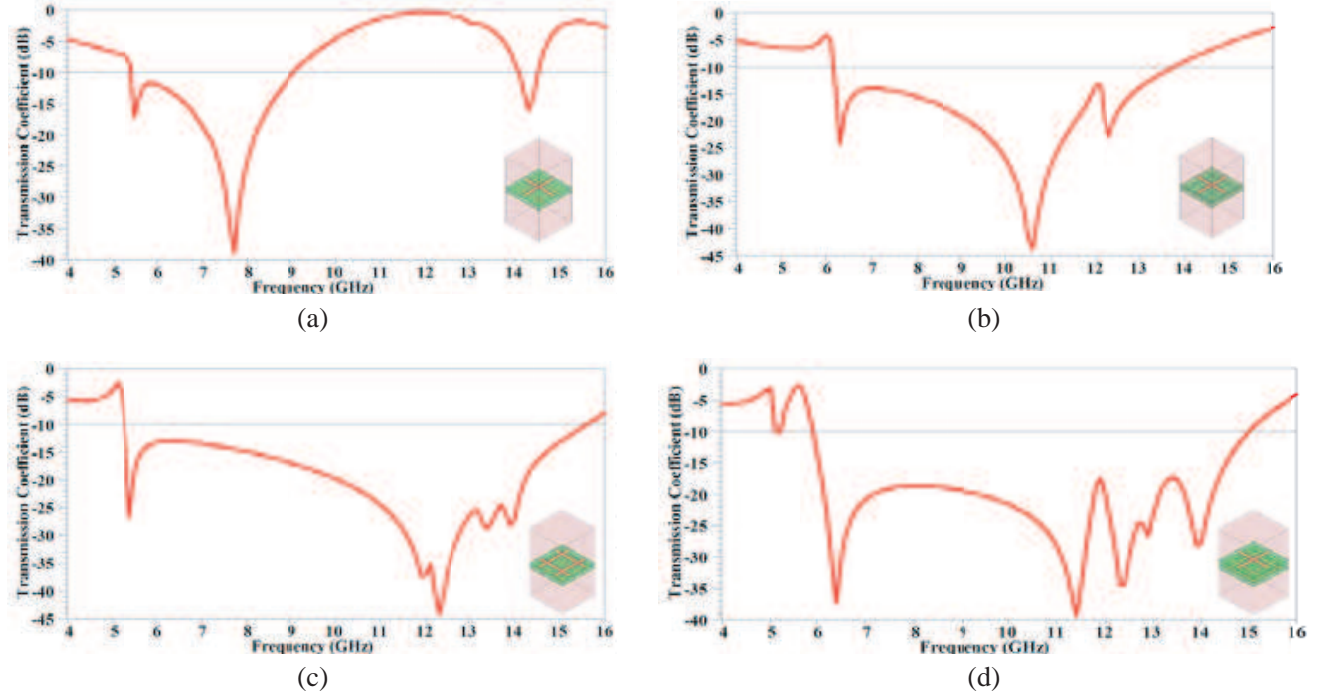


Figure 5. Simulated transmission characteristics of cascaded layers, (a) layer I-II, (b) layer I-III, (c) layer II-III, (d) layer I-II-III.

Table 1. Parameters obtained from various layers.

Layers	Start Freq (GHz)	Stop Freq (GHz)	Resonant Freq (GHz)	Bandwidth	% age Bandwidth	S_{21}
Layer I	5.9	7.0	6.4	1.1 GHz	17.0	-30.5
Layer II	5.5	7.9	6.8	2.4 GHz	35.8	-36.0
			14.3	14.9	14.6	600 MHz
Layer III	6.6	15.2	11.3	8.6 GHz	78.8	-44.0
Layer I-II	5.4	9.0	5.5	3.6 GHz	50	-17.0
			7.6			-39.0
			14.0	14.5	14.3	500 MHz
Layer I-III	6.1	13.7	6.4	7.6 GHz	76.7	-26.0
			10.6			-35.0
			12.1			-43.0
Layer II-III	5.2	15.6	5.4	10.4 GHz	100	-27.0
			12.2			-44.0
Layer I-II-III	6.0	15.0	6.4	9.0 GHz	85.7	-37.0
			11.4			-39.0
			12.4			-34.0
			14.0			-29.0

cell at 6.4 GHz. For layer II at lower resonating frequency of 6.8 GHz, the current distribution stays on the inner side of horizontal arms of the unit cell whereas at the higher resonating frequency (14.6 GHz) there is little radiation. Layer III at resonating frequency of 11.3 GHz radiates strongly on the inner side of upper horizontal arms, and the current flow decreases down the lower horizontal arms of the

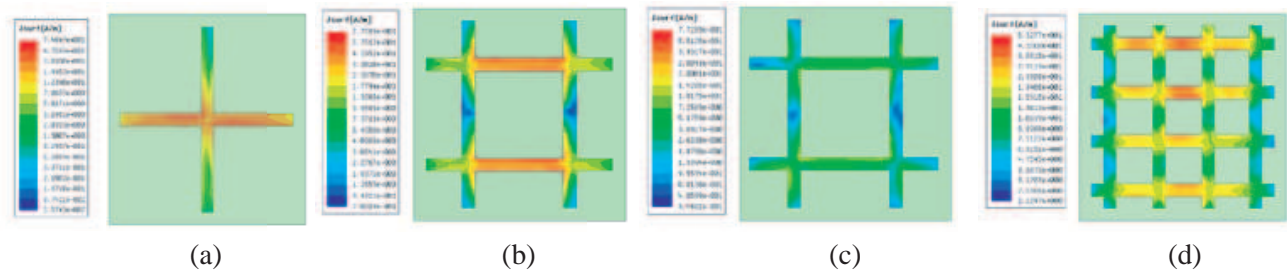


Figure 6. Surface current distribution, (a) layer I at 6.4 GHz, (b) layer II at 6.8 GHz and 14.6 GHz, (c) layer III at 11.3 GHz.

unit cell.

$$\text{Arm length} = \frac{c_0}{4 \cdot f \sqrt{(\epsilon_r + 1)/2}} \tag{1}$$

3. PARAMETRIC ANALYSIS

The structure discussed so far has three layers of FSS, with best results obtained for wide stopband in the case when layer II and layer III are cascaded at 1 mm spacing. The parametric analysis is done on the FSS to obtain well optimized results. The analyses are: a) Different layers of FSS on single dielectric. b) Layers kept in face-to-face position. c) Layers in cascading mode at different spacings.

3.1. Different Layers of FSS on Single Dielectric

Figure 7 shows different combinations of layers on single dielectric, i.e., single FR4. When layer I and layer II are combined on a single FR4, a stopband of bandwidth of 3.4 GHz is obtained. Combination of layer I and layer III produces a much wider stopband of 8.8 GHz. Layer II and layer III add another

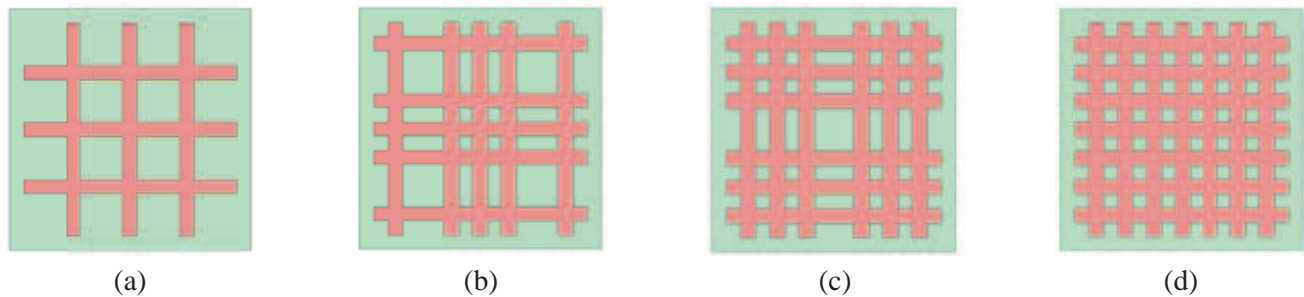


Figure 7. Single dielectric layers, (a) layer I-II, (b) layer I-III, (c) layer II-III, (d) layer I-II-III.

Table 2. Bandwidth (in GHz) with separate/single dielectric and face-to-face case.

Layers	Bandwidth (GHz) with Seperate Dielectric	Bandwidth (GHz) with Single Dielectric	Bandwidth (GHz) with Face-to-Face Layers
I-II	3.6	3.4	3.2
I-III	9.4	8.8	9.8
II-III	10.4	9.6	10.2
I-II-III	9.0	9.6	--

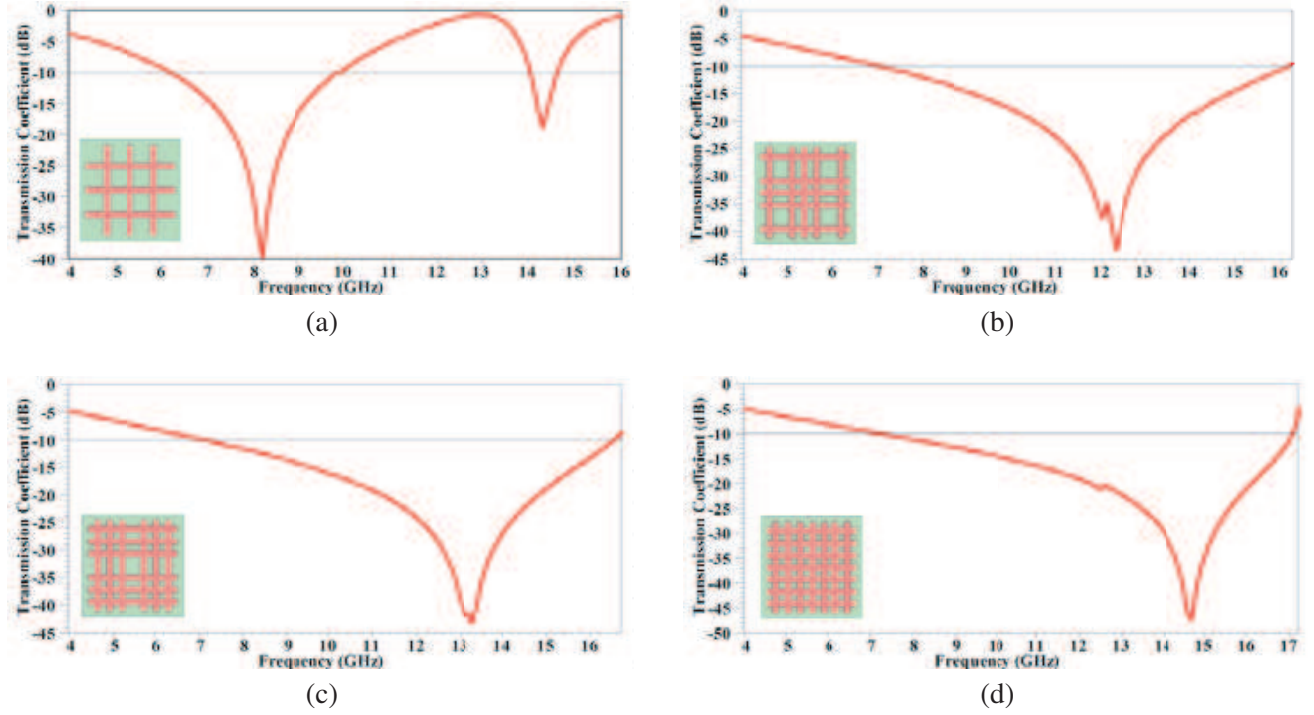


Figure 8. Simulated transmission coefficients of layers on single dielectric, (a) layer I-II, (b) layer I-III, (c) layer II-III, (d) layer I-II-III.

800 MHz of stopband to previous case; fetching overall stopband of 9.6 GHz. When all the layers are etched on single FR4, a similar value of stopband (9.6 GHz) is achieved. Simulation results are shown in Fig. 8. Table 2 shows the comparison obtained in bandwidths of earlier simulated results with the results obtained in the case of single dielectric. The table clearly shows that the bandwidth of stopbands in the case of layers etched on separate dielectrics has an edge over the bandwidth of stopbands in the case of single dielectric. Layer II-III provides the maximum value of stopband. Hence, for further parametric study layers etched on separate dielectrics will be considered.

3.2. Layers Kept in Face-to-Face Position

The layers studied in Section 2 assume that the layers are kept back-to-back or are in cascaded form. When these layers are kept face-to-face, the simulation results are depicted in Fig. 9, which show that here also layer II and layer III, when kept in face-to-face condition, provide a wide stopband of 10.2 GHz. However, the bandwidth here lags by a factor of 200 MHz in comparison to the case of cascaded form. Table 2 depicts the results of two parametric studies. The results show that the layers should be kept in cascaded mode for wider stopbands.

Table 3. Bandwidth (in GHz) obtained for different spacing between layers.

Layers with Spacing	Bandwidth (in GHz)				
	$\lambda/48$	$\lambda/24$	$\lambda/12$	$\lambda/8$	$\lambda/4$
I-II	3.2	3.6	3.3	3.4	3.2
I-III	9.8	9.6	9.6	10.1	11.2
II-III	10.6	10.4	10.2	10.2	10.0
I-II-III	9.0	9.0	10.0	10.2	10.0

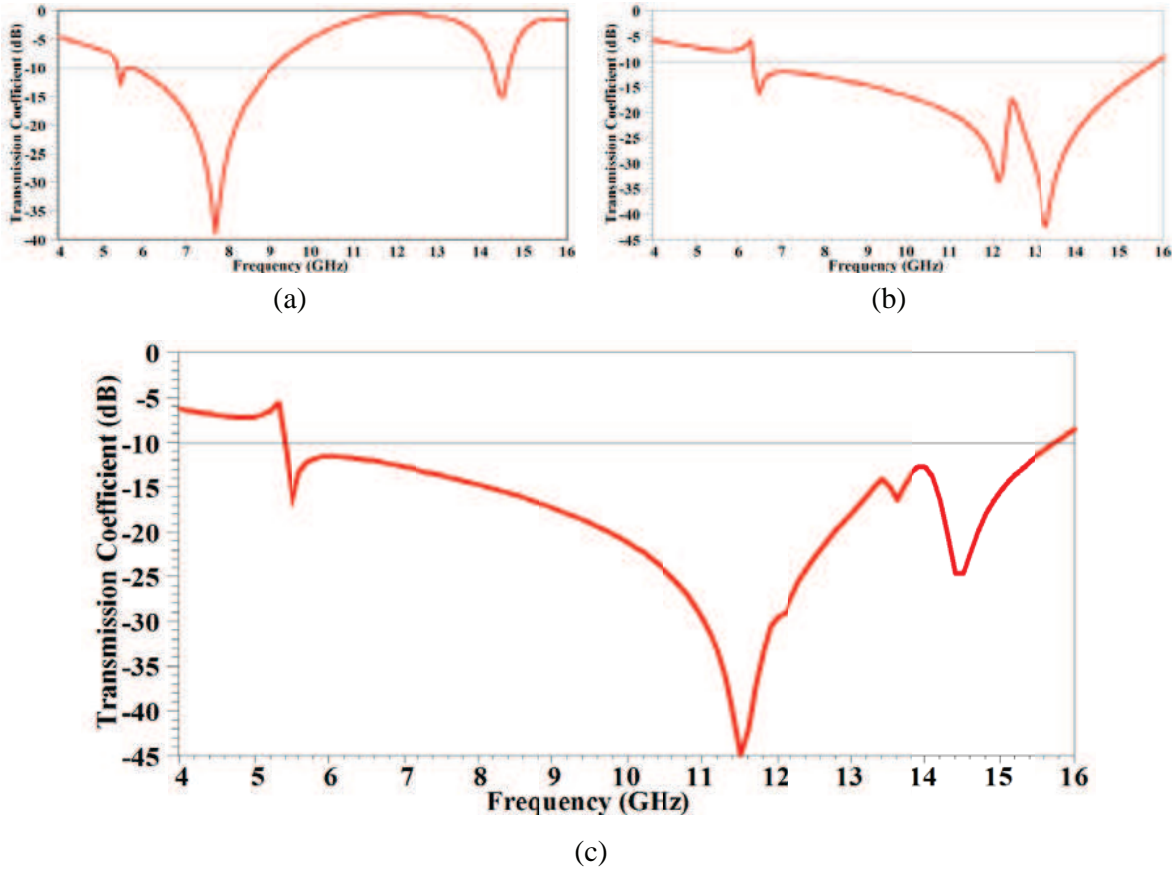


Figure 9. Simulated transmission coefficients for face-to-face scenario, (a) layer I-layer II, (b) layer I-layer III, (c) layer II-layer III.

3.3. Layers in Cascading Mode at Different Spacings

The analysis of layers done so far studies the layers in cascade mode at 1 mm ($\lambda/24$) spacing w.r.t. each other. Now simulation is carried out when spacing is varied in between the layers (central frequency, $f_c = 12.2$ GHz). The results are shown in Fig. 10. Table 3 depicts that at $\lambda/48$ spacing, layer II-III produces 10.6 GHz of wide stopband. As the spacing between layers increases, layer II-III remains consistent in reflecting the 4G/X-band/Ku-band as desired.

Hence, the parametric study reveals that for obtaining wide stopband, out of all designs investigated, combination of layer II and layer III can be used in cascade configuration at $\lambda/24$ spacing between them.

Table 4. Comparison of proposed design with existing designs.

Parameter	Ref. [5]	Ref. [14]	Proposed
Frequency Band	4–7 GHz	8–11 GHz	5–16 GHz
Unit cell (mm)	11 × 11	13 × 13	15 × 15
Number of layers	2	2	2
Layer spacing (mm)	4	7.4	1
% Bandwidth	54%	45%	100%
Approach used	Cascading	Cascading	Cascading

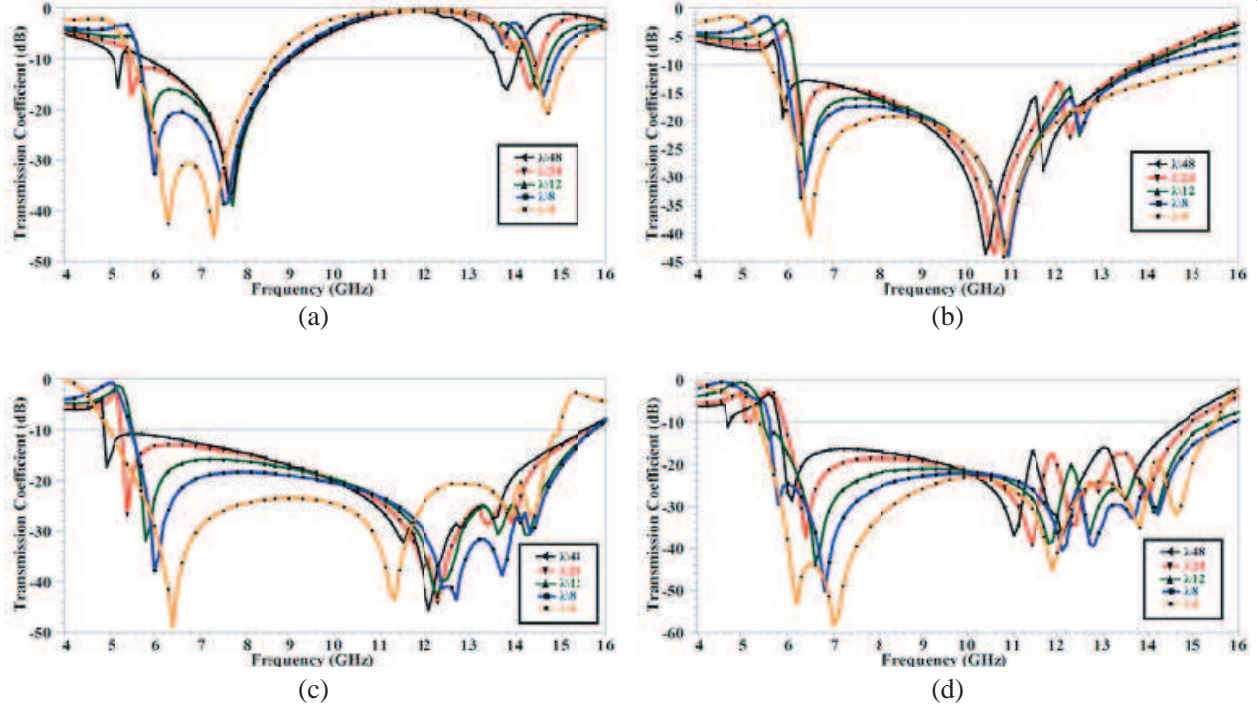


Figure 10. Simulated transmission coefficients of layers at various spacings.

4. EXPERIMENTAL RESULTS

In order to validate the simulated results, the proposed FSS was fabricated on an FR4 panel. A prototype of 100 unit cells per layer of layer II and layer III respectively is fabricated as shown in Fig. 11. The measurement setup is made using signal generator, power meter, two standard gain horn antennas, and the fabricated panel is placed between them. Fig. 12 illustrates the comparison of measured results from the experimental setup and simulated results from the software. They are in good agreement with each other which justifies the proposed methodology. The little variation in the measured results is due to the edge reflections and scattering of EM waves at the time of measurement. Table 4 shows the comparison of performance of proposed design with already existing designs [5, 14]. It is clear from the table that a comparatively wider stopband is obtained from the proposed design in comparison to [5] and [14]. The percentage bandwidth obtained from the proposed FSS is 100% (almost double that of existing designs). The layer spacing is also very small in the proposed design.



Figure 11. Fabricated prototype.

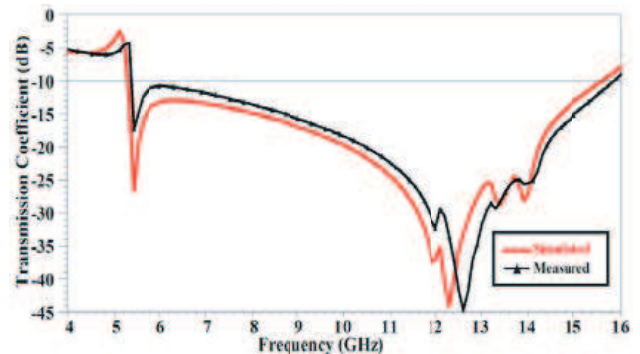


Figure 12. Comparison of transmission coefficients of measured and simulated results.

5. CONCLUSION

In this paper, a cascaded dual-layer wideband FSS reflector resonating at 5.2–15.6 GHz is presented. The percentage bandwidth obtained with the prototype structure in the proposed frequency range is 100% (almost double that of quoted designs). The advantages of this reflector are wide stopband of 10.4 GHz and simplicity of the design. The reflector marks its application in 4G, X-band and Ku-band. A prototype of a dual-layer FSS is fabricated, and the fabrication results agree well with the simulation results hence justifying the methodology of the proposed design.

REFERENCES

1. Munk, B. A., *Selective Surfaces: Theory and Design*, Wiley, New York, 2000.
2. Munk, B. A., *Finite Antenna Arrays and FSS*, John Wiley and Sons, Inc., 2005.
3. Zhu, H., Y. Yu, X. Li, and B. Li, "A wideband and high gain dual-polarized antenna design by a frequency selective surface for a WLAN applications," *Progress In Electromagnetics Research C*, Vol. 54, 57–66, 2014.
4. Zhong, T., H. Zhang, X.-L. Min, Q. Chen, and G.-C. Wu, "Wideband frequency selective surface with a sharp band edge based on mushroom-like cavity," *Progress In Electromagnetics Research Letters*, Vol. 62, 105–110, 2016.
5. Chatterjee, A. and S. Parui, "A dual layer frequency selective surface reflector for wideband applications," *Radio Engg.*, Vol. 25, No. 1, 67–72, 2016.
6. Ang, B.-K. and B.-K. Chung, "A wideband E-shaped microstrip patch antenna for 5–6 GHz wireless communications," *Progress In Electromagnetics Research*, Vol. 75, 397–407, 2007.
7. Kesavan, A., R. Karimian, and T. Denidni, "A novel wideband frequency selective surface for millimeter-wave applications," *IEEE Anten. and Wireless Propag. Lett.*, Vol. 15, 1711–1714, 2016.
8. Izquierdo, B., J. Robertson, and E. A. Parker, "Wideband FSS for electromagnetic architecture in buildings," *Journ. of Material Science and Progress, Appl. Phys. A*, 771–774, 2011.
9. Pirhadi, A., H. Bahrami, and J. Nasri, "Wideband high directive aperture coupled microstrip antenna design by using a FSS superstrate layer," *IEEE Trans. on Antennas and Propag.*, Vol. 60, No. 4, 2101–2106, 2012.
10. Sivasami, R., B. Moorthy, M. Kanagasabai, V. Samsingh, and M. Alsath, "A wideband frequency tunable fss for electromagnetic shielding applications," *IEEE Trans. on Electromag. Comp.*, Vol. 60, No. 1, 280–284, 2018.
11. Zhang, L., G. Yang, Q. Wu, and J. Hua, "A novel active frequency selective surface with wideband tuning range for EMC purpose," *IEEE Trans. on Magnetics*, Vol. 48, No. 11, 4534–4537, 2012.
12. Pasian, M., S. Monni, A. Neto, M. Ettore, and G. Gerini, "Frequency selective surfaces for extended bandwidth backing reflector functions," *IEEE Trans. on Antennas and Propag.*, Vol. 58, No. 1, 43–50, 2010.
13. Moustafa, L. and B. Jecko, "Design and realization of a wide-band EBG antenna based on FSS and operating in the Ku-band," *International Jour. of Antennas and Propag.*, Vol. 2010, 1–8, 2010.
14. Lins, H., E. Barreto, and A. D'assuncao, "Enhanced wideband performance of coupled frequency selective surfaces using metaheuristics," *Micro. and Opt. Techno. Lett.*, Vol. 55, No. 4, 711–715, 2013.
15. Braz, E. and A. Campos, "Dual/wide band multifractal frequency selective surface for applications in S and X band," *Micro. and Opt. Techno. Lett.*, Vol. 56, No. 10, 2217–2222, 2013.
16. Azemi, S. N., K. Ghorbani, and W. S. T. Rowe, "3D frequency selective surfaces with wideband response in antenna technology," *Small Antennas, Novel EM Structures and Materials, and Applications (IWAT)*, IEEE, 212–215.
17. Liu, Y., L. Zhou, and J. Ouyang, "A bandpass circular polarization frequency selective surface with wideband rejection properties," *IEEE International Symposium on Antennas and Propag. & USNC/URSI National Radio Science Meeting*, 275–276, 2017.